

## Article

# Effects of Different Variables on the Formation of Mesopores in Y Zeolite by the Action of CTA<sup>+</sup> Surfactant

Juliana F. Silva, Edilene Deise Ferracine and Dilson Cardoso \* 

Catalysis Laboratory LabCat, Department of Chemical Engineering, Federal University of São Carlos, P.O. Box 676, São Carlos SP CEP 13.565-905, Brazil; julianafloriano75@gmail.com (J.F.S.); edilenedeise@ufscar.br (E.D.F.)

\* Correspondence: dilson@ufscar.br; Tel.: +55-016-3351-8693

Received: 25 June 2018; Accepted: 26 July 2018; Published: 4 August 2018



**Abstract:** Zeolites are microporous crystalline aluminosilicates with a number of useful properties including acidity, hydrothermal stability, and structural selectivity. However, the exclusive presence of micropores restricts diffusive mass transport and reduces the access of large molecules to active sites. In order to resolve this problem, mesopores can be created in the zeolite, combining the advantages of microporous and mesoporous materials. In this work, mesopores were created in the Ultrastable USY zeolite (silicon/aluminum ratio of 15) using alkaline treatment (NaOH) in the presence of cetyltrimethylammonium bromide surfactant, followed by hydrothermal treatment. The effects of the different concentrations of NaOH and the surfactant on the textural, chemical, and morphological characteristics of the modified zeolites were evaluated. Generating mesoporosity in the USY zeolite was possible through the simultaneous presence of surfactant and alkaline solution. Among the parameters studied, the concentration of the alkaline medium had the greatest influence on the textural properties of the zeolites. The presence of Cetyltrimethylammonium Bromide (CTA<sup>+</sup>) prevented the amorphization of the structure during the modification and also avoided desilication of the zeolite.

**Keywords:** zeolites; mesopores; diffusion; surfactant

## 1. Introduction

Zeolites are a class of natural and synthetic minerals that have several structural characteristics in common based on three-dimensional combinations of tetrahedra (TO<sub>4</sub>, where T represents atoms of silicon and aluminum) connected by oxygen atoms [1].

The microporous zeolite structure is responsible for the acidity, hydrothermal stability, and structural selectivity of these materials [2]. However, the exclusive presence of micropores limits diffusive mass transport and reduces the access of large molecules to the active sites [3,4]. One method for resolving this problem is creating mesopores in the zeolite structure to combine the properties of microporous and mesoporous zeolites in a single material.

Ultrastable USY is a synthetic zeolite widely used in the petroleum industry. This zeolite is not directly obtained by hydrothermal synthesis, but instead by vapor treatment of Y zeolite. This process creates mesopores that do not significantly affect intra-crystalline diffusion, since they mainly exist as cavities that are connected to the surface by micropores [5,6]. This means that the preparation of USY zeolite possessing secondary porosity has to be performed via post-synthesis modifications.

Compared to conventional zeolites, zeolites with mesopores provide high molecular weight reagents greater access to the active sites. They have shorter retention times of reaction products in

the micropores, avoiding secondary reactions and improving selectivity toward the primary products of interest. Furthermore, relative to purely mesoporous materials, they exhibit better hydrothermal stability and higher acidity [7].

The strategies that have been developed to create mesoporosity in zeolites can be grouped into constructive and destructive techniques. In the constructive approach (bottom-up), the mesopores are created during the synthesis of the zeolite, with or without the use of templates. In the destructive route (top-down), mesopores are produced by means of post-synthesis treatments, such as dealumination and desilication. The modification of zeolites using surfactants together with alkaline treatment for the formation of mesoporosity is a highly attractive post-synthesis route, since it produces materials with controlled mesoporosity in terms of the shape, size, connectivity, and location of the mesopores [5,8].

Different approaches have been described for the creation of mesoporosity using surfactants. The recrystallization technique reported by Ivanova et al. [9] involves two stages: the zeolite is first partially destroyed using an alkaline treatment, then the surfactant is added to the reaction mixture, and hydrothermal treatment is applied. This work investigated the creation of mesopores in mordenite (MOR) zeolite using the recrystallization method. Modification of MOR (Si/Al = 49) was performed by treatment with NaOH at room temperature, followed by hydrothermal treatment at 100 °C, in the presence of cetyltrimethylammonium bromide (CTAB). The materials obtained under the conditions used, which were classified as micro- and mesoporous composites, were tested in a transalkylation reaction of biphenyl (BP) with para-diisopropyl benzene (p-DIPB) and in the cracking reaction of 1,3,5-triisopropylbenzene (TIPB). Each of these reactions required a certain volume of mesopores to ensure enhanced performance.

Another approach reported in the literature is alkaline treatment in the presence of a CTAB surfactant at room temperature, followed by heating of the mixture at 150 °C for several hours to rearrange the structure and create ordered mesopores in the zeolite [8,10,11]. The advantage of this technique, compared to the recrystallization method, is that it avoids complete amorphization of the zeolite by the surfactant, which can occur during more severe alkaline treatments [5].

The crystal rearrangement associated with the use of a surfactant during alkaline treatment was first reported in a patent published in 2005 by Garcia-Martínez [12]. This technique, described as surfactant-templating, was introduced to reduce the difficulty of preparing zeolites with mesopores, instead of materials composed of distinct regions (one mesoporous and the other zeolitic).

USY zeolites with low contents of aluminum are sensitive to treatment with alkaline solution and readily undergo amorphization. For this reason, organic cations such as TPA<sup>+</sup>, TMA<sup>+</sup>, and CTA<sup>+</sup> alkylammonium cations can be used in the alkaline solution in order to preserve the micropore volume and the associated properties of the zeolite [13,14].

In this work, USY zeolite (Si/Al = 15) was modified by alkaline treatment in the presence of CTAB surfactant, with subsequent hydrothermal treatment to form a substantial volume of mesopores. The main objective was to investigate the effects of different alkaline medium and surfactant concentrations on the structural, textural, and chemical properties of zeolites with mesopores, as well as to evaluate the role of the surfactant during modification.

## 2. Materials and Methods

### 2.1. USY Zeolite Modification

The USY zeolite used as the starting material (code CBV720; SiO<sub>2</sub>/Al<sub>2</sub>O<sub>3</sub> = 30) was manufactured by Zeolyst (Conshohocken, PA, USA). The molar ratio of the reaction mixture employed in the zeolite modification was 0.0052 HY:x Na<sub>2</sub>O:100 H<sub>2</sub>O:y CTAB. The values for the base (x) and surfactant (y) are shown in Table 1.

**Table 1.** Modification conditions used for preparation of the materials.

Sample	Base Molar Ratio (x)	Surfactant Molar Ratio (y)
YB0-S0.1	0	0.1
YB0.02-S0.1	0.02	0.1
YB0.04-S0.1	0.04	0.1
YB0.06-S0.1	0.06	0.1
YB0.08-S0.1	0.08	0.1
YB0.08-S0	0.08	0
YB0.08-S0.02	0.08	0.02
YB0.08-S0.04	0.08	0.04
YB0.08-S0.06	0.08	0.06
YB0.08-S0.08	0.08	0.08

To prepare the reaction mixture with molar ratio of 0.0052 HY:0.08 Na<sub>2</sub>O:100 H<sub>2</sub>O:0.1 CTAB, 0.60 g of CTAB was dissolved in 30 mL of aqueous 0.085 mol/L NaOH solution, followed by addition of 1 g USY zeolite under agitation for 20 min. Subsequently, the reaction mixture was subjected to hydrothermal treatment for 20 h at 150 °C in an autoclave. The suspension was filtered and the solid material obtained was washed until pH 7 and dried at 80 °C. Calcination was then performed in a muffle furnace at 550 °C for 8 h, using a heating rate of 2 °C/min. The samples were labeled using the nomenclature YBx-Sy.

## 2.2. Influence of Surfactant

The zeolites denoted YB0.04-S0-60/6h and YB0.04-S0.08-60/6h were prepared as described in Section 2.1. employing the following molar ratios: 0.0052 HY:0.04 Na<sub>2</sub>O:100 H<sub>2</sub>O:0 CTAB, and 0.0052 HY:0.04 Na<sub>2</sub>O:100 H<sub>2</sub>O:0.08 CTAB, respectively. The hydrothermal treatment temperature was 60 °C and the treatment duration was 6 h. A third sample, denoted YB0.04-CTA<sup>+</sup>-60/6h, was prepared using a reaction mixture with the molar ratio 0.0052 HY:0.04 Na<sub>2</sub>O:100 H<sub>2</sub>O:0 CTAB. For the preparation of the sample named YB0.04-CTA<sup>+</sup>-60/6h, an ion exchange was first performed with the original zeolite USY by using its mixture with an aqueous solution of CTAB with a concentration of 0.2 mol/L. The ratio used was 1 g zeolite to 100 mL solution. Three consecutive exchanges of 1 h each were performed. At the end of each exchange, the zeolite was washed with distilled water, and after drying it was oven dried at 80 °C. Subsequently, 1 g zeolite containing CTA<sup>+</sup> cations that compensated the negative charges in the structure was dissolved in 30 mL of aqueous 0.0045 mol/L NaOH solution under agitation for 20 min. Afterward, the reaction mixture was submitted to hydrothermal treatment for 6 h at 60 °C in an autoclave. The suspension was filtered and the solid material obtained was washed until pH 7 and dried at 80 °C. Calcination was then performed in a muffle furnace at 550 °C for 8 h using a heating rate of 2 °C/min.

The difference, relative to the zeolites prepared as described above, was that the initial zeolite contained CTA<sup>+</sup> cations that compensated for the negative charges of the zeolite structure. The hydrothermal treatment was performed for 6 h at 60 °C.

## 2.3. Characterization

X-ray diffractograms were acquired using a Rigaku MiniFlex 600 diffractometer (Tokyo, Japan) operated with Cu K $\alpha$  radiation ( $\lambda = 1.5418 \text{ \AA}$ ). The relative crystallinity (RC) was determined using the ratio of the sums of the peak areas at 23.3°, 26.6°, and 30.9° 2 $\theta$  for the modified samples, relative to the original sample, as recommended by ASTM. The original zeolite was considered as a standard, with an assumed crystallinity of 100%.

The textural properties of the zeolites were evaluated using nitrogen physisorption isotherms acquired using a Micromeritics ASAP 2020 system. The mesopore diameter distribution was determined by the Barret-Joiner-Halenda (BJH) method, employing the desorption branch of the

isotherm. The micropore volume was determined by the t-plot method, using a 0.3–0.5 nm thickness interval. The mesopore volume was determined by the NLDFT method for pores with cylindrical geometry based on the functional density [10,15]. The total quantities of acid sites in the materials were determined by the Ammonia Temperature Programmed Desorption technique (TPD-NH<sub>3</sub>), employing a Micromeritics AutoChem II 2920 chemisorption analyzer.

The global silicon/aluminum ratios were determined by energy dispersive spectroscopy (EDS). The analyses were performed using a field emission gun (FEG) electron microscope operated at 20 kV with the samples dispersed on double-sided adhesive carbon tapes.

Quantification of silicon in the filtrate was performed by chemical analysis using an Optima 8000 Inductively Coupled Plasma Optical Emission Spectrometer (ICP-OES).

Analysis of the zeolites by <sup>27</sup>Al nuclear magnetic resonance (NMR) was performed using a Bruker Avance III-400 system operated with a 9.4 T magnetic field. The samples were packed into zirconia rotors with external diameter of 4 mm and the measurements were performed at a temperature of 23 °C.

### 3. Results

#### 3.1. Influence of Surfactant Concentration

The X-ray diffractograms of the modified zeolites and the original USY zeolite (Figure 1) revealed that only the zeolite modified without the addition of a surfactant (YB0.08-S0) did not show diffraction peaks corresponding to the FAU structure.

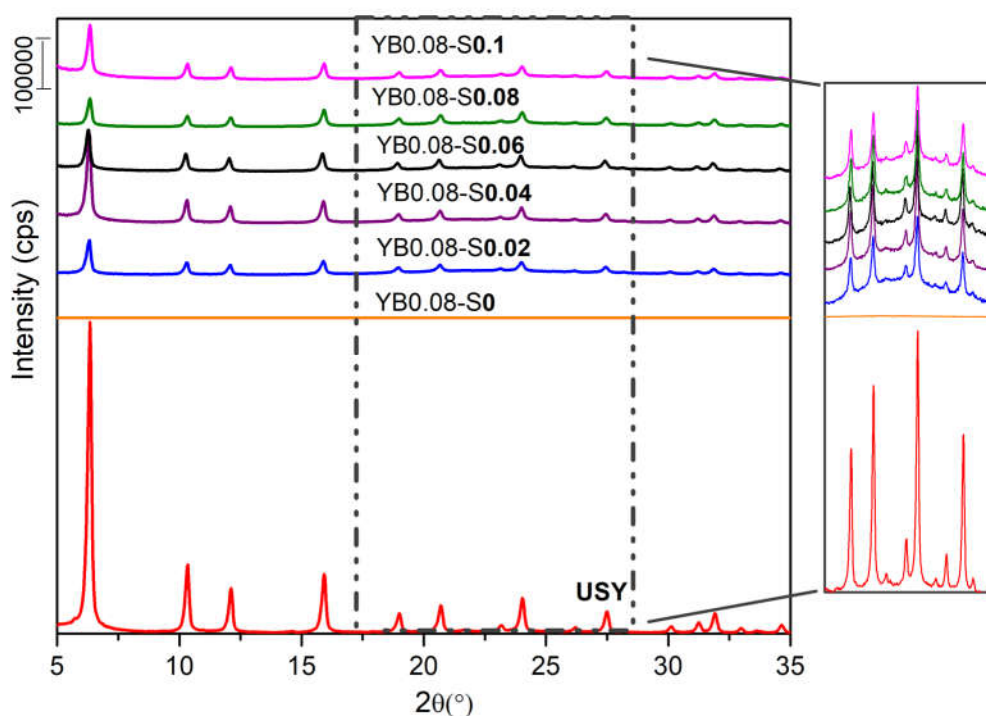


**Figure 1.** X-ray diffractograms of the samples modified using different concentrations of cetyltrimethylammonium bromide (CTAB).

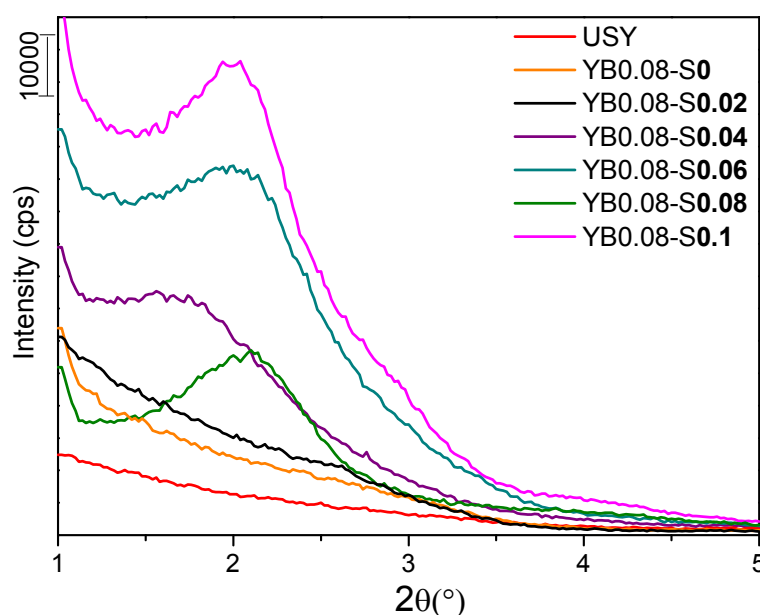
Calculation of the relative crystallinity (RC) of the modified zeolites (Table 2) revealed an average reduction in RC of approximately 65% under the conditions tested. Notably, the use of CTA<sup>+</sup> in the alkaline treatment protected the Si–O–Si bonds from attack by hydroxyl groups (OH<sup>−</sup>), thus preventing the complete destruction of the zeolite structure. In a study on the desilicalization of zeolite Y with different Si/Al ratios used in this study, the same behavior in the presence of CTAB was verified [14].

**Table 2.** Relative crystallinity (RC) and textural properties of the modified zeolites, according to the amount of surfactant used during the modification.

Sample	RC (%)	$V_{\text{total}}^1$ (cm <sup>3</sup> /g)	$V_{\text{micro}}^2$ (cm <sup>3</sup> /g)	$V_{\text{meso}}^3$ (cm <sup>3</sup> /g)	$S_{\text{ext}}^2$ (cm <sup>2</sup> /g)
USY	100	0.395	0.239	0.115	208
YB0.08-S0	0	0.023	0.002	0.033	20
YB0.08-S0.02	32	0.225	0.087	0.123	165
YB0.08-S0.04	39	0.395	0.107	0.193	364
YB0.08-S0.06	38	0.468	0.091	0.265	536
YB0.08-S0.08	38	0.603	0.092	0.363	597
YB0.08-S0.1	33	0.649	0.077	0.404	661

<sup>1</sup>  $P/P_0 = 0.85$ ; <sup>2</sup> External surface area by t-plot; <sup>3</sup> determined by NLDFT. The pH of the reaction mixture after the USY treatment was about 11.0.

The X-ray diffractograms showed the presence of a halo around 15–30° 2 $\theta$  (the magnification in Figure 1), possibly due to silicon atoms removed from the structure and deposited in the form of amorphous silica organized by the CTA<sup>+</sup> micelles. For a better visualization of the amorphous halo in the X-ray diffraction (XRD) pattern of sample YB0.08-S0, the graph was plotted on a smaller scale. (Figure S1). At small angles, the X-ray diffractograms of the modified zeolites showed a peak near of 2° 2 $\theta$ , corresponding to the repetition of crystallographic planes, possibly resulting from the ordering of pores larger than 2 nm, derived from the treatments of the materials (Figure 2).

**Figure 2.** X-ray diffractograms at small angles of the modified zeolites produced using different concentrations of surfactant (CTA<sup>+</sup>).

Comparison of the modified zeolites with low ( $y = 0.02$ ) and high ( $y = 0.1$ ) surfactant contents showed that the relative crystallinity did not change significantly. In other words, the surfactant content did not considerably influence this parameter.

The initial USY zeolite presented a type I isotherm (Figure 3) according to the IUPAC [16] classification, reflecting a predominance of micropores in its structure. However, the modified materials showed isotherms that were a combination of types I and IV (Figure 3), indicative of the presence of micro- and mesopores in their structures and confirming the effectiveness of the modifications. The porous structure of the YB0.08-S0 zeolite was completely destroyed due to the absence of CTA<sup>+</sup>

during the modification, in agreement with the destruction of the faujasite structure shown by the X-ray diffraction analysis (Figure 1).

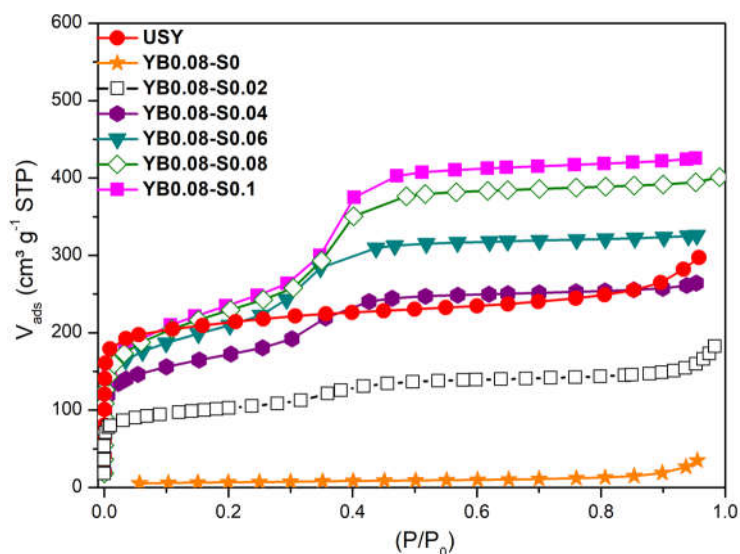


**Figure 3.** N<sub>2</sub> physisorption isotherms for the original USY zeolite and the modified zeolites produced using different surfactant concentrations.

The larger mesopore volume of the modified samples produced using higher surfactant ratios (Table 2) were probably due to the formation of a higher number of micelles, since these are templates for the formation of mesopores. The external area, determined by the t-plot method, increased with increasing mesopore volume.

Figure 4 shows the volumes of micropores and mesopores as a function of the surfactant ratio used in modification of the original USY zeolite. In the absence of addition of CTA<sup>+</sup>, the volume of micro- and mesopores was almost zero because the crystalline structure had been completely destroyed, as shown previously. Addition of the CTA<sup>+</sup> surfactant at different concentrations resulted in an almost constant micropore volume, in agreement with the effect on the relative crystallinity, described previously.

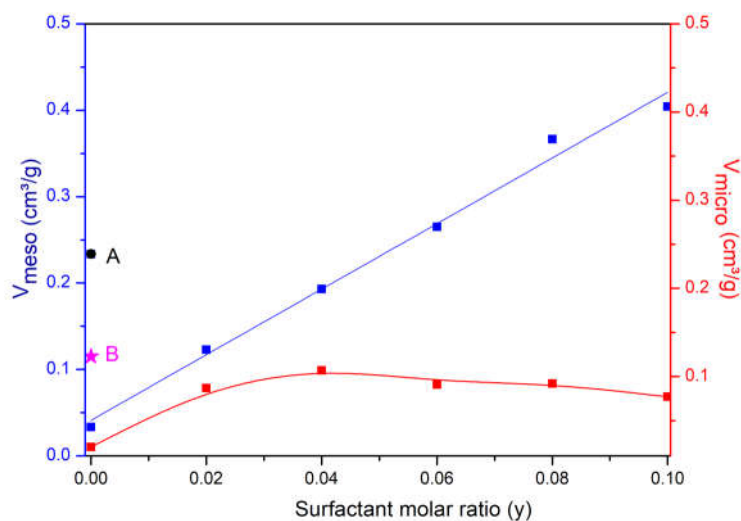


**Figure 4.** Micropore and mesopore volumes, as a function of surfactant molar ratio. A and B represent the volume of micropores and mesopores in the original USY zeolite, respectively.



The original sample possessed a small quantity of pores with diameters around 3.8 nm, derived from the hydrothermal treatment applied to the Y zeolite to increase its catalytic stability (Figure 5). Modification of the USY zeolite using the lowest surfactant concentration ( $\gamma = 0.02$ ) maintained part of the original pores but led to the formation of smaller mesopores around 3 nm in size. The use of higher surfactant concentrations led to the disappearance of pores of around 3.8 nm, but increased the amount of mesopores around 3.0 nm in size. Given that the diameters of CTA<sup>+</sup> cation micelles are in the range 3 to 4 nm [7], the formation of mesopores in this same size range could be attributed to the role of the surfactant as a template in the formation of mesopores.

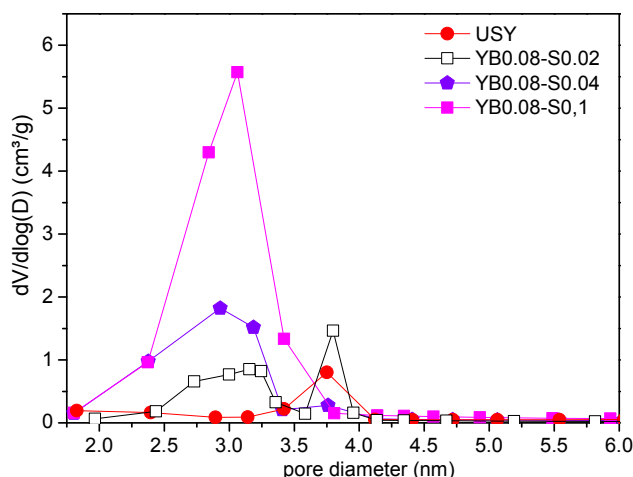


**Figure 5.** Pore diameter distributions (Barret-Joiner-Halenda method; BJH) of the modified zeolites produced using different CTAB concentrations.

### 3.2. Influence of Base Concentration

The X-ray diffractograms of the modified USY zeolites presented diffraction peaks characteristic of the faujasite structure, but with lower intensity compared to the diffractogram of the original USY zeolite (Figure 6). The X-ray diffractograms of the modified zeolites produced using higher amounts of base ( $x = 0.04$ – $0.08$ ) with a more pronounced halo at  $2\theta$  of  $15$ – $30^\circ$ , possibly related to amorphous silica, different from the X-ray diffractograms of the modified zeolites produced with lower base content.

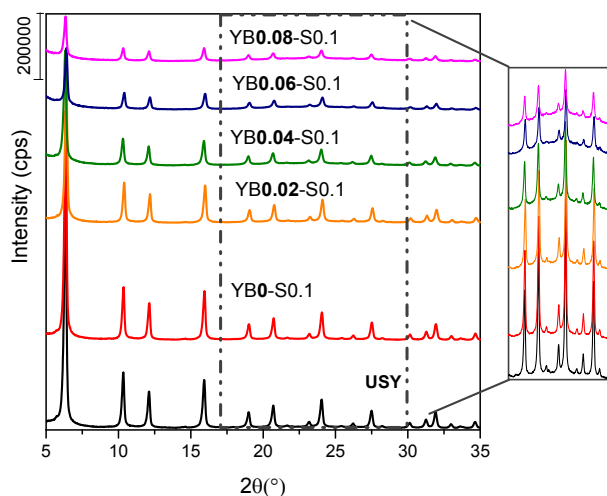


**Figure 6.** X-ray diffractograms of the modified zeolites produced using different base ratios.

The relative crystallinity of the zeolites decreased as the concentration of the alkaline medium increased (Table 3). This demonstrated the importance of adjusting the concentration of the alkali solution in order to avoid excessive amorphization of the material and conserve the properties of the zeolite.

**Table 3.** Relative crystallinity and textural properties of the modified zeolites, according to the base concentration used.

Sample	RC (%)	$V_{\text{total}}^1$ (cm <sup>3</sup> /g)	$V_{\text{micro}}^2$ (cm <sup>3</sup> /g)	$V_{\text{meso}}^3$ (cm <sup>3</sup> /g)	$S_{\text{ext}}^2$ (cm <sup>3</sup> /g)	pH <sup>4</sup>
USY	100	0.395	0.239	0.115	208	-
YB0-S0.1	96	0.396	0.242	0.142	186	3
YB0.02-S0.1	80	0.367	0.199	0.170	209	9
YB0.04-S0.1	52	0.464	0.129	0.229	420	10
YB0.06-S0.1	38	0.627	0.095	0.379	591	11
YB0.08-S0.1	33	0.649	0.077	0.404	661	11

<sup>1</sup>  $P/P_0 = 0.85$ ; <sup>2</sup> t-plot; <sup>3</sup> NLDFT; <sup>4</sup> pH of the reaction mixture after the USY treatment.

The X-ray diffractograms at small angles of the modified zeolites produced using different base concentrations are shown in Figure 7. The YB0-S0.1, YB0.02-S0.1, and original USY zeolites did not present a diffraction peak at  $2^\circ 2\theta$ , corresponding to the repetition of the crystallographic planes, probably due to the absence of mesoporosity with a certain degree of organization.

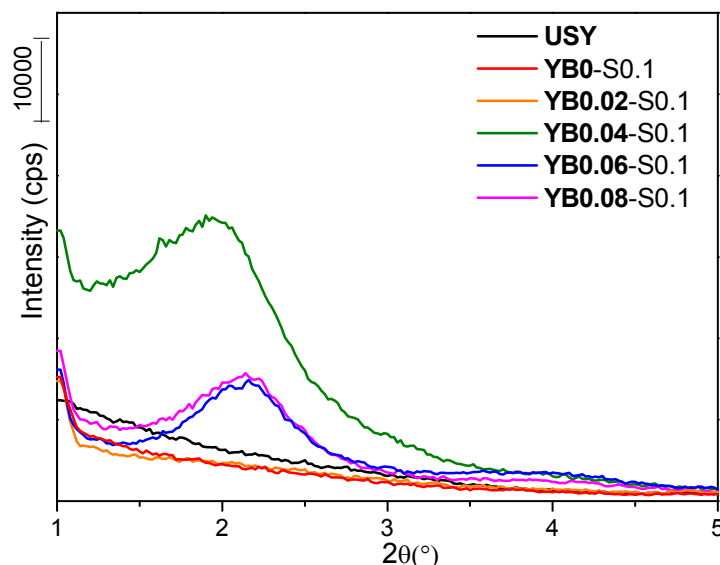


**Figure 7.** X-ray diffractograms at small angles of the modified zeolites produced using different base concentrations.

The nitrogen adsorption isotherms (Figure 8) revealed the lower nitrogen adsorption by the YB0.02-S0.1 zeolite at a relative pressure of 0.4, indicative of the generation of fewer mesopores due to the milder alkaline treatment. The modified zeolites produced using higher base concentrations presented greater mesopore formation.



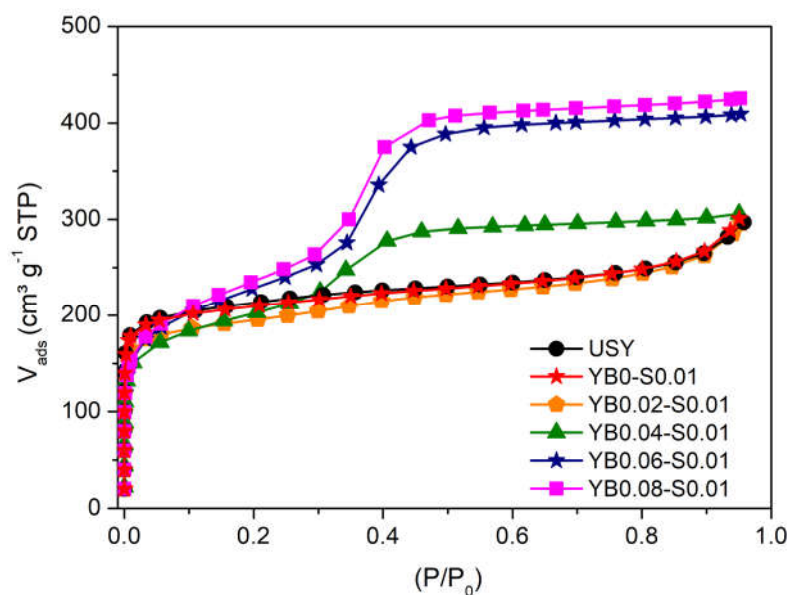


**Figure 8.** Nitrogen adsorption isotherms of the modified samples produced using different concentrations of the alkaline medium.

From the data presented in Table 3 and Figure 8, no mesoporosity was created when the modification was performed in the absence of a base. This indicated that the formation of  $\text{SiO}^-$  species by breaking the Si–O–Si bonds due to the action of a base was fundamental for the formation of mesopores.

A positive correlation was found between the NaOH concentration used in the treatment and the mesopore volume of the resulting material. In addition, an increase in the volume of mesopores was accompanied by a decrease in the micropore volume (Table 3, Figure 9), as also found elsewhere [10].

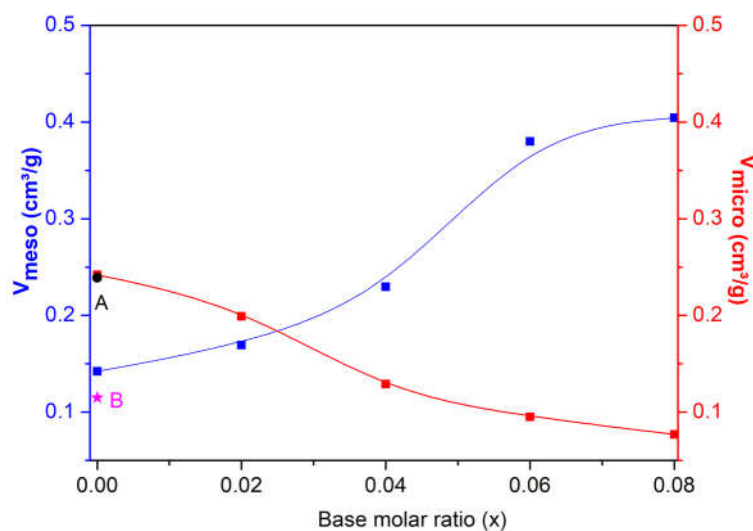


**Figure 9.** Zeolite mesopore and micropore volumes as a function of the base ratio ( $x$ ) used for the modification. A and B represent the volume of micropores and mesopores in the original USY zeolite, respectively.

The modified zeolites demonstrated a narrow pore size distribution centered near 3 nm (Figure 10). As the alkaline treatment concentration increased, the volume of the mesopores generated also

increased. The mildest alkaline treatment ( $x = 0.02$ ) was insufficient to create any substantial quantity of mesopores templated by the  $\text{CTA}^+$  micelles.

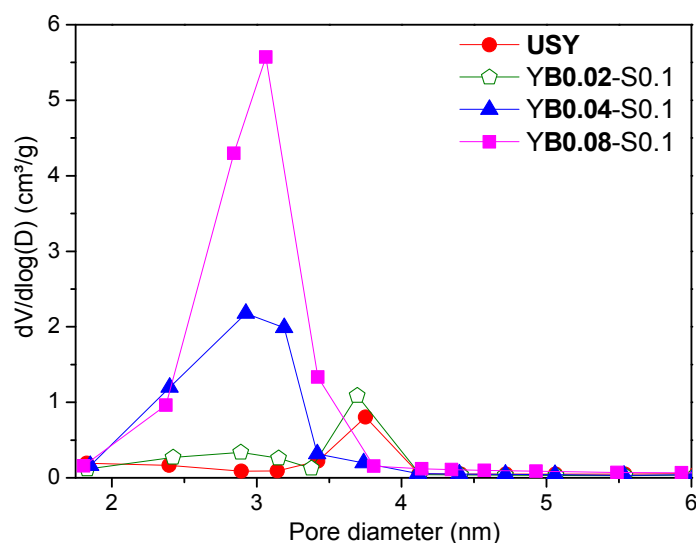


**Figure 10.** Pore size distributions obtained using the BJH method applied to the isotherms (desorption branch) for the original zeolite and the modified zeolites produced using different base concentrations.

The observed main influence on the modification of the textural properties of the zeolites by the concentration of the alkaline medium was further investigated via chemical analyses of the materials.

The different chemical environments of the aluminum in the zeolites were investigated by  $^{27}\text{Al}$  NMR (Figure 11). The signal corresponding to octahedral aluminum ( $\text{Al}^{\text{VI}}$ ) was observed at 0 ppm, whereas tetracoordinated aluminum ( $\text{Al}^{\text{IV}}$ ) was identified both within and outside the zeolitic structure, as shown by signals located at 60 and 53 ppm, respectively. The spectra indicated that the use of a higher NaOH concentration led to a decrease in the tetracoordinated aluminum in the zeolite structure, accompanied by an increase in non-structural or distorted tetracoordinated aluminum, as reported previously [17].

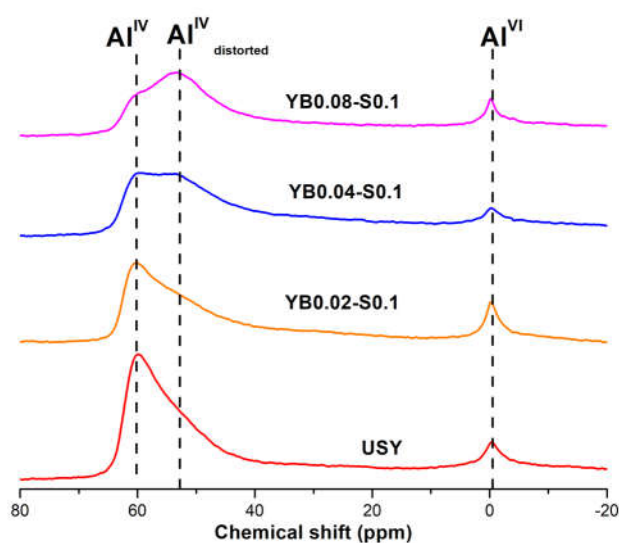


**Figure 11.**  $^{27}\text{Al}$  nuclear magnetic resonance (NMR) spectra of the calcined modified zeolites produced using different alkaline medium concentrations.

This change in the chemical environment of the aluminum led to a decrease in Brønsted acid sites, since these sites are generated due to the presence of tetrahedral aluminum in the zeolite structure. The presence of distorted or external (outside the structure) tetracoordinated aluminum generates Lewis acid sites [17,18].

The TPD-NH<sub>3</sub> profiles (Figure 12) showed two peaks: the first around 208–217 °C and the second around 325–360 °C. The peak at the lower temperature could be attributed to the release of weakly adsorbed NH<sub>3</sub>, whereas the peak at the higher temperature could be explained by the release of NH<sub>3</sub> from NH<sub>4</sub><sup>+</sup> bound at stronger acid sites [19,20].

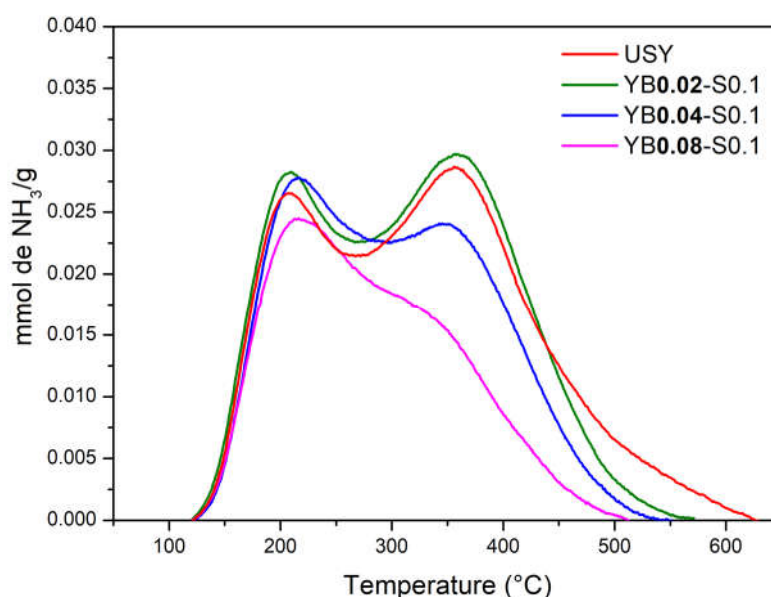


**Figure 12.** TPD-NH<sub>3</sub> profiles of the calcined original zeolite and the zeolites produced using different base concentrations.

Considering the total amounts of ammonia desorbed at higher temperatures (Table 4), the original USY zeolite contained a greater quantity of acid sites compared to the modified zeolites, demonstrating that the process used to create mesoporosity resulted in fewer acid sites [2,10].

**Table 4.** Quantification of the total acidity of the zeolites.

Sample	T (°C)	NH <sub>3</sub> ( $\frac{\mu\text{mol}}{\text{g}}$ )	NH <sub>3</sub> (total) ( $\frac{\mu\text{mol}}{\text{g}}$ )	Si/Al
USY	209	101	547	14
	358	446		
YB0.02-S0.1	208	144	535	15
	358	391		
YB0.04-S0.1	216	115	462	14
	350	347		
YB0.08-S0.1	216	99	344	14
	325	245		

A yield of 97.6% was obtained for the modification performed under the most severe conditions ( $x = 0.08$ ,  $y = 0.1$ ). ICP analysis showed that the amount of silicon present in the filtrate was insignificant and corresponded to only 0.07% of the silicon present in the original zeolite. This was supported by the constancy of the global Si/Al ratio (Table 4), confirming that the modification led to no significant

loss of silicon contained in the material. The Si removed from the structure by the alkaline treatment was subsequently associated with the surfactant micelles and was recrystallized.

### 3.3. Effect of the Presence of the Surfactant

We evaluated the influence of the presence of the CTA<sup>+</sup> surfactant during modification of the USY zeolite on the generation of mesopores. As observed in Section 3.2., the presence of the surfactant during the alkaline treatment protected the zeolite structure from more intense action of the NaOH. The X-ray diffractograms of the YB0.04-S0.08-60/6h and YB0.04-S0-60/6h zeolites presented characteristic peaks of the faujasite structure (Figure 13).

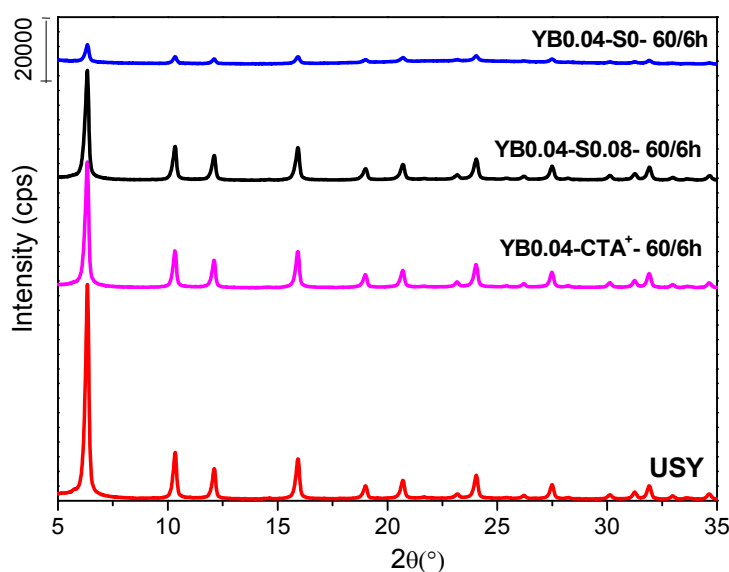


**Figure 13.** X-ray diffractograms of the zeolites used to study the influence of the presence of CTA<sup>+</sup> cations.

The zeolite modified without the presence of CTA<sup>+</sup> (YB0.04-S0-60/6h) showed a 77% reduction of relative crystallinity, whereas the RC of the zeolite modified with the addition of CTA<sup>+</sup> in the reaction mixture (YB0.04-S0.08-60/6h) decreased by only 6% (Table 5), confirming the protective effect of the surfactant.

**Table 5.** Relative crystallinity and textural properties of the zeolites used to study the effect of the presence of the CTA<sup>+</sup> cations.

Sample	RC(%)	V <sub>total</sub> <sup>1</sup> (cm <sup>3</sup> /g)	V <sub>micro</sub> <sup>2</sup> (cm <sup>3</sup> /g)	V <sub>meso</sub> <sup>3</sup> (cm <sup>3</sup> /g)	S <sub>ext</sub> <sup>2</sup> (cm <sup>3</sup> /g)
USY	100	0.395	0.239	0.156	208
YB0.04-CTA <sup>+</sup> -60/6h	98	0.405	0.245	0.160	179
YB0.04-S0.08-60/6h	94	0.426	0.240	0.186	233
YB0.04-S0-60/6h	23	0.355	0.084	0.271	334

<sup>1</sup> P/P<sub>0</sub> = 0.85; <sup>2</sup> t-plot; <sup>3</sup> NLDFT.

The modified USY zeolite produced using CTA<sup>+</sup> cations to compensate for the negative charges of the aluminum (denoted YB0.04-CTA<sup>+</sup>-60/6h) exhibited high relative crystallinity (Table 5, Figure 13). To verify the presence of the CTA<sup>+</sup> cations in this sample, thermogravimetric analysis (TGA) was performed (Figure S4). The presence of the cations could be explained by the presence of the cetyl (-C<sub>16</sub>H<sub>33</sub>) and methyl (-CH<sub>3</sub>) groups of the surfactant, whose occupation of space prevented the hydroxyl (OH<sup>-</sup>) groups from disrupting the Si–O–Si bonds protecting the micropores. This explanation

was supported by a previous study that reported that the use of tetramethylammonium hydroxide (TMAOH) [14] could protect the zeolite structure from hydroxyl attack, different from the use of the inorganic bases  $\text{NH}_4\text{OH}$  and  $\text{NaOH}$ .

Analysis of the isotherms (Figure 14) revealed a smaller pore volume of the zeolite modified under mild conditions in the absence of the  $\text{CTA}^+$  cation (YB0.04-S0-60/6h) compared to the zeolites modified in the presence of the surfactant. This occurred because the  $\text{CTA}^+$  cations were not present to protect the zeolite structure, so the action of the base disrupted a greater quantity of Si–O–Si bonds.

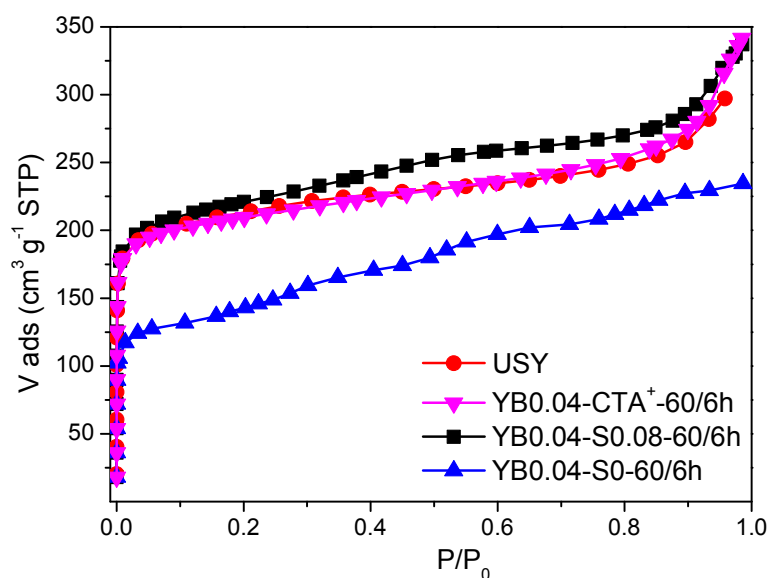


**Figure 14.** Nitrogen adsorption isotherms for the zeolite samples used to evaluate the effect of the presence of  $\text{CTA}^+$ .

Analysis of the textural properties of the zeolites (Table 5) showed that the zeolite produced with  $\text{CTA}^+$  cations compensating for the charges of the structure (YB0.04- $\text{CTA}^+$ -60/6h) did not form mesopores after the modification. This could be explained by the absence of micelle formation during the process, given that no surfactant was added to the reaction mixture.

Analysis of the textural properties of the zeolite modified in the presence of the surfactant under milder hydrothermal treatment conditions (YB0.04-S0.08-60/6h) revealed that the milder alkaline solution and hydrothermal treatment conditions, when used together, were insufficient to form a significant quantity of mesopores. In this case, the micropore and mesopore volumes were virtually identical to those of the original USY zeolite (Table 5).

In the absence of the surfactant, mesopores formed with a concomitant reduction in micropores (Table 5). This likely occurred because the absence of  $\text{CTA}^+$  cations facilitated the breaking of the Si–O–Si bonds, with mesopores being formed by desilication, even with the use of mild reaction conditions.

#### 4. Conclusions

The proposed methodology was effective for the creation of mesopores in USY zeolite in the presence of  $\text{CTA}^+$  cations. The presence of the  $\text{CTA}^+$  cations was fundamental in the modification process, since the cations hindered the attack by hydroxyl ( $\text{OH}^-$ ) groups, avoiding the dissolution of the zeolite crystals during the modification.

The use of an alkaline treatment was essential, since the absence of the base resulted in the lack of mesoporosity creation. Therefore, mesoporosity formation in the USY zeolite required the simultaneous presence of the alkaline medium and the  $\text{CTA}^+$  surfactant.

In addition to the protective effect of the CTA<sup>+</sup> surfactant, an increase in its concentration had a positive effect on increasing the mesopore volume of the modified zeolites, without reducing the relative crystallinity, different than the behavior observed following variation of the alkaline medium concentration. A higher concentration of the alkaline medium significantly influenced the textural properties and the relative crystallinity values of the modified zeolites.

The total quantities of acid sites of the modified zeolites were lower than for the original USY zeolite. Increasing the alkaline medium concentration used in the modification resulted in lower acidity due to the substantial decrease in the micropore volume. This reduction in the quantity of acid sites could be attributed to changes in the chemical environments of aluminum.

The USY zeolite with Si/Al = 15 was highly sensitive to desilication, preventing the formation of a substantial volume of mesopores without amorphization or even total destruction of the zeolite structure. Therefore, the methodology described here is attractive, as it is a versatile technique that increases the mesopore volume, without risking loss of the zeolitic structure.

**Supplementary Materials:** The following are available online at <http://www.mdpi.com/2076-3417/8/8/1299/s1>, Figure S1: X-ray diffractograms of the sample YB0.08-S0, Figure S2: Nitrogen adsorption (closed symbols) and desorption (open desorption) isotherms at 77 K of the modified samples produced using different concentrations surfactant, Figure S3: Nitrogen adsorption (closed symbols) and desorption (open desorption) isotherms at 77 K of the modified samples produced using different concentrations of the alkaline medium, Figure S4: Thermogravimetric analysis of the sample original USY and YB0.04-CTA+-60/6h.

**Author Contributions:** J.F.S. and D.C. designed the experiments; E.D.F. and J.F.S. performed the experimental work; J.F.S., E.D.F., and D.C. analyzed the data; D.C. provided reagents, materials, and analysis tools; J.F.S. wrote the article, with contributions from D.C. and E.D.F.

**Funding:** This research received no external funding.

**Acknowledgments:** The authors are grateful to CAPES/MEC for scholarship support.

**Conflicts of Interest:** The authors declare no conflicts of interest.

## References

- Giannetto, G. *Zeolitas: Características, Propiedades y Aplicaciones Industriales*, 1st ed.; Editorial Innovación Tecnológica: Caracas, Venezuela, 1990; p. 170.
- Chal, R.; Cacciaguerra, T.; van Donk, S.; Gérardin, C. Pseudomorphic synthesis of mesoporous zeolite Y crystals. *Chem. Commun.* **2010**, *46*, 7840–7842. [[CrossRef](#)] [[PubMed](#)]
- Pérez-Ramírez, J.; Christensen, C.H.; Egeblad, K.; Christensen, C.H.; Groen, J.C. Hierarchical zeolites: Enhanced utilisation of microporous crystals in catalysis by advances in materials design. *Chem. Soc. Rev.* **2008**, *37*, 2530–2542. [[CrossRef](#)] [[PubMed](#)]
- Verboekend, D.; Nuttens, N.; Locus, R.; Van Aelst, J.; Verolme, P.; Groen, J.C.; Pérez-Ramírez, J.; Sels, B.F. Synthesis, characterisation, and catalytic evaluation of hierarchical faujasite zeolites: Milestones, challenges, and future directions. *Chem. Soc. Rev.* **2016**, *45*, 3331–3352. [[CrossRef](#)] [[PubMed](#)]
- Li, K.; Valla, J.; Garcia-Martinez, J. Realizing the commercial potential of hierarchical zeolites: New opportunities in catalytic cracking. *Chem. Cat. Chem.* **2014**, *6*, 46–66.
- Koster, A.J.; Ziese, U.; Verkleij, A.J.; Janssen, A.H.; de Jong, K.P. Three-dimensional transmission electron microscopy: A novel imaging and characterization technique with nanometer scale resolution for Materials Science. *J. Phys. Chem. B* **2000**, *104*, 9368–9370. [[CrossRef](#)]
- Ivanova, I.I.; Kasyanov, I.A.; Maerle, A.A.; Zaikovskii, V.I. Mechanistic study of zeolites recrystallization into micro-mesoporous materials. *Microporous Mesoporous Mater.* **2014**, *189*, 163–172. [[CrossRef](#)]
- García-Martínez, J.; Johnson, M.; Valla, J.; Li, K.; Ying, J.Y. Mesostructured zeolite Y—high hydrothermal stability and superior FCC catalytic performance. *Catal. Sci. Technol.* **2012**, *2*, 987–994. [[CrossRef](#)]
- Ivanova, I.I.; Kuznetsov, A.S.; Ponomareva, O.A.; Yuschenko, V.V.; Knyazeva, E.E. Micro/mesoporous catalysts obtained by recrystallization of mordenite. In *Studies in Surface Science and Catalysis*; Elsevier: Amsterdam, The Netherlands, 2005; pp. 121–128.



10. Sachse, A.; Grau-Atienza, A.; Jardim, E.O.; Linares, N.; Thommes, M.; García-Martínez, J. Development of intracrystalline mesoporosity in zeolites through surfactant-templating. *Cryst. Growth Des.* **2017**, *17*, 4289–4305. [[CrossRef](#)]
11. Sachse, A.; Wuttke, C.; Díaz, U.; de Souza, M.O. Mesoporous Y zeolite through ionic liquid based surfactant templating. *Microporous Mesoporous Mater.* **2015**, *217*, 81–86. [[CrossRef](#)]
12. Ying, Y.; García-Martínez, J. Mesoporous Zeolitic Materials, and Methods of Making and Using the Same. U.S. Patent 20050239634A1, 27 October 2005.
13. Verboekend, D.; Vilé, G.; Pérez-Ramírez, J. Mesopore formation in USY and beta zeolites by base leaching: Selection criteria and optimization of pore-directing agents. *Cryst. Growth Des.* **2012**, *12*, 3123–3132. [[CrossRef](#)]
14. Shutkina, O.V.; Knyazeva, E.E.; Ivanova, I.I. Preparation and physicochemical and catalytic properties of micro-mesoporous catalysts based on faujasite. *Pet. Chem.* **2016**, *56*, 138–145. [[CrossRef](#)]
15. Thomas, J.M.; Leary, R.K. A Major Advance in Characterizing Nanoporous Solids Using a Complementary Triad of Existing Techniques *Angew. Chemistry* **2014**, *53*, 12020–12021.
16. Sing, K.S.W.; Everett, D.H.; Haul, R.A.W.; Moscou, L.; Pierotti, R.A.; Rouquerol, J.; Siemieniewska, T. Reporting physisorption data for gas/solid systems with special reference to the determination of surface area and porosity. *Pure Appl. Chem.* **1985**, *57*, 603–619. [[CrossRef](#)]
17. Van Aelst, J.; Verboekend, D.; Philippaerts, A.; Nuttens, N.; Kurttepel, M.; Gobechiya, E.; Haouas, M.; Sree, S.P.; Denayer, J.F.M.; Martens, J.A.; et al. Catalyst design by  $\text{NH}_4\text{OH}$  treatment of USY zeolite. *Adv. Funct. Mater.* **2015**, *25*, 7130–7144. [[CrossRef](#)]
18. Peters, A.W.; Wu, C.C. Selectivity effects of a new aluminum species in strongly dealuminated USY containing FCC catalysts. *Catal. Lett.* **1995**, *30*, 171–179. [[CrossRef](#)]
19. Katada, N.; Igi, H.; Kim, J.-H. Determination of the acidic properties of zeolite by theoretical analysis of temperature-programmed desorption of ammonia based on adsorption equilibrium. *J. Phys. Chem. B* **1997**, *101*, 5969–5977. [[CrossRef](#)]
20. Niwa, M.; Katada, N. New method for the temperature-programmed desorption (TPD) of ammonia experiment for characterization of zeolite acidity: A review: TPD of ammonia for characterization of zeolite acidity. *Chem. Rec.* **2013**, *13*, 432–455. [[CrossRef](#)] [[PubMed](#)]



© 2018 by the authors. Licensee MDPI, Basel, Switzerland. This article is an open access article distributed under the terms and conditions of the Creative Commons Attribution (CC BY) license (<http://creativecommons.org/licenses/by/4.0/>).